International Journal of Thermal Sciences 48 (2009) 1823–1828

Contents lists available at ScienceDirect

International Journal of Thermal Sciences

journal homepage: www.elsevier.com/locate/ijts

# Cycle parameter optimization of vortex tube expansion transcritical $CO_2$ system

Jahar Sarkar*

*Department of Mechanical Engineering, Institute of Technology, BHU, Varanasi, UP 221005, India*

ARTICLE INFO

*Article history:*
Received 7 November 2007
Received in revised form
22 January 2009
Accepted 22 January 2009
Available online 17 March 2009

*Keywords:*
Vortex tube
Transcritical $CO_2$ cycle
Modelling
Optimization
COP improvement

ABSTRACT

Optimization studies along with optimum parameter correlations are presented in this article for a vortex tube expansion transcritical $CO_2$ refrigeration cycle with two cycle layouts based on the Maurer model (1999) and the Keller model (1997). A simple thermodynamic model is proposed and used for vortex tube analysis. Finally, the COP improvement and effect on optimum discharge pressure by using vortex tube in transcritical $CO_2$ cycle instead of expansion valve are presented. The results show that the effect of cold mass fraction and inlet water temperature to desuperheater (used to cool hot gas from vortex tube) on the cycle optimization is negligible. The Maurer model is better than the Keller model in terms of moderately more COP improvement and lower cost due to less components. The use of a vortex tube is more effective for higher gas cooler exit temperature for both models. Results show that the vortex tube expansion transcritical $CO_2$ cycle for the Maurer model can give higher COP improvement for lower cooling temperature applications; however the trend is reverse for the Keller model.



## 1. Introduction

Use of vortex tube as an expansion device in transcritical $CO_2$ cycle seems to be one of the promising cycle modifications to improve the system performance [1,2]. The vortex tube was basically developed for the gas expansion, working on the Ranque–Hilsch effect and lot of experimental and numerical works on that have been reported [3]. Although, according to recent research results, the Ranque–Hilsch principle also works when the liquid is expanded through vortex tube providing a sufficient high rate of pressure difference [4]. Hooper and Ambrose [5] first experimentally attempted to increase the refrigerating effect of a vapor refrigerator using a special version of Ranque–Hilsch vortex tube replacing the throttling valve. Collins and Lovelace [6] experimentally studied the expansion of two-phase propane through the Ranque–Hilsch tube. Other scientists have started to examine the principle behind the vortex tube expansion device in refrigeration systems in 1990s and proposed various refrigeration cycle configurations using vortex tube as expansion device. The COP improvements by using vortex tube were reported for the refrigerants R22, R134a, propane, ammonia, and carbon dioxide through German examinations [4].

Recently, Li et al. [7] performed a thermodynamic analysis of different expansion devices for the transcritical $CO_2$ cycle. A vortex tube expansion device and an expansion work output device were proposed to recover the expansion losses. The maximum increase in COP using a vortex tube or expansion work output device, assuming ideal expansion process, was about 37% compared to the one using an isenthalpic expansion process at evaporation temperature of 5 °C and gas cooler exit temperature of 40 °C. The increase in COP reduced to about 20% when the efficiency for the expansion work output device was 0.5. In order to achieve the same improvement in COP using a vortex tube expansion device, the efficiency of the vortex tube (ratio of enthalpy drop of cold mass to the isentropic enthalpy drop of total mass) had to be above 0.38. Christensen et al. [4] used CFD modelling for analysis of $CO_2$ expansion vortex tube. Although the extensive analyses on the optimization of compressor discharge pressure for different cycle configurations using vortex tube as expansion device are scarce in open literature.

In the present study, the extensive analyses have been done on the optimization of compressor discharge pressure based on the maximum cooling COP for the vortex tube expansion transcritical $CO_2$ refrigeration cycle with two different cycle layouts: one is based on the Maurer model [8] and another is based on the Keller model [9]. For the analysis of vortex tube, a simple thermodynamic model has been used. Finally the improvement of cooling COP of transcritical $CO_2$ cycle by using vortex tube instead of expansion valve and also the effect on optimum discharge pressure have been presented for both the cycle layouts.

## 2. Vortex tube expansion transcritical $CO_2$ cycle

Two layouts have been used in the present study: Maurer model (1999) [8] and Keller Model (1997) [9]. As the separation effect is

* Tel.: +91 9919787557.
*E-mail address:* js_iitkgp@yahoo.co.in

1290-0729/$ – see front matter © 2009 Elsevier Masson SAS. All rights reserved.
doi:10.1016/j.ijthermalsci.2009.01.016

**Nomenclature**

| | |
|---|---|
| COP | coefficient of performance (–) |
| $h$ | specific enthalpy (kJ kg$^{-1}$) |
| $p$ | pressure (MPa) |
| $q$ | cooling/heating effect (kJ kg$^{-1}$) |
| $t$ | temperature (°C) |
| $w$ | specific work (kJ kg$^{-1}$) |
| $x$ | vapor quality (–) |
| $y$ | cold mass fraction (–) |
| ΔCOP | improvement of COP (%) |
| $\varepsilon$ | heat exchanger effectiveness (–) |
| $\eta$ | isentropic efficiency (%) |

*Subscript*

| | |
|---|---|
| $b$ | basic cycle |
| $c$ | compressor |
| $co$ | gas cooler exit |
| $d$ | compressor discharge |
| $ev$ | evaporator |
| $n$ | vortex tube nozzle |
| $opt$ | optimum |
| $wi$ | water inlet to desuperheater |

negligible for pure liquid, Maurer model is very effective for carbon dioxide, where the expansion mostly takes place from the supercritical state due low critical temperature, not from the liquid phase. As shown in Figs. 1 and 2, in the vortex tube, the gas is expanding from gas cooler pressure to evaporation pressure and divided into three fractions: saturated liquid (state 4), which is collected in a ring inside the vortex tube (100% separation efficiency), saturated vapor (state C) and superheated gas (state H), which are created because of the Ranque–Hilsch effect. The saturated liquid and vapor are mixed again (state 6) and going through the evaporator to give useful cooling effect. The superheated gas is cooled in the heat exchanger (desuperheater) to state 5 and mixed with the gas coming from the evaporator (state 7) before entering the compressor (state 1).

For the Keller model, as shown in Figs. 3 and 4, the liquid is evaporated in a two-stage expansion, since it is difficult to get liquid separation with vortex tube. The refrigerant is cooled in an intermediate cooler from state 3 to state 4. The refrigerant is then expanded to an intermediate pressure through a throttle valve and to a liquid separator, where the vapor is separated to state 8 from the liquid at state 5. The vapor is then superheated to state 9 in the

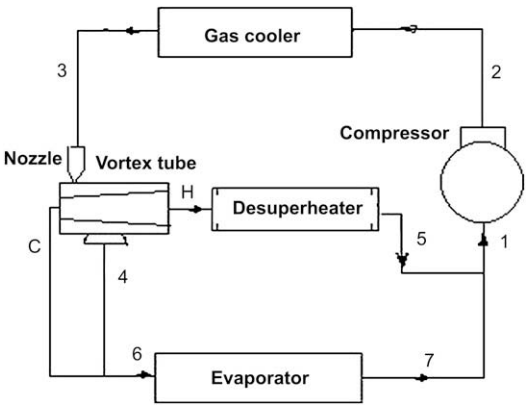


**Fig. 1.** Cycle layout of vortex tube expansion cycle for Maurer model.

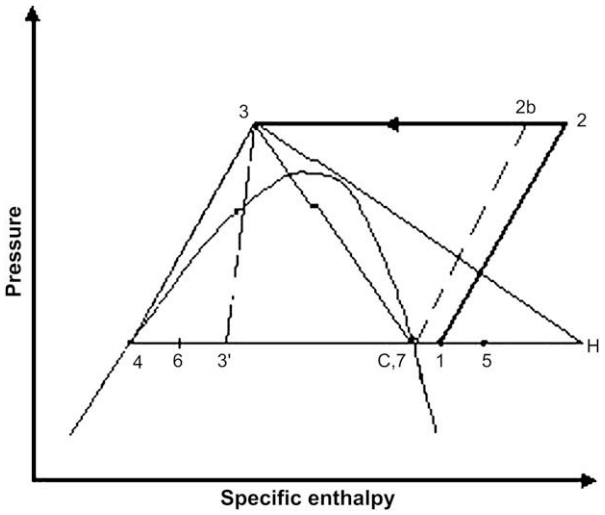


**Fig. 2.** p-h diagram of vortex tube expansion cycle for Maurer model.

intermediate cooler and is expanded through the vortex tube, where it separates in a cold (state C) and warm (state H) fraction. The warm fraction must be warmer than the ambient to get advantage of the vortex tube. The warm fraction is then cooled to state 10 in a desuperheater and then mixed with the cold outlet of the vortex tube. The mixture is then mixed with the vapor from evaporator (state 7) before entering the compressor (state 1). It can be noted that the Keller model is modified slightly (exit of desuperheater and cold stream is connected to evaporator outlet instead of inlet) in this study. For both cycle layouts, the pressure drop through the vortex tube is controlled by adjusting the geometric parameters of vortex tube as well as expansion nozzle or controlling the needle valves used at vortex tube outlets.

## 3. Thermodynamic model

For the thermodynamic model, Keller used the first and second laws of thermodynamics to describe the vortex tube but no clarification is available how the isentropic efficiency is related to specific entropy production and Maurer used conservation of mass, first and second laws of thermodynamics but neglecting entropy

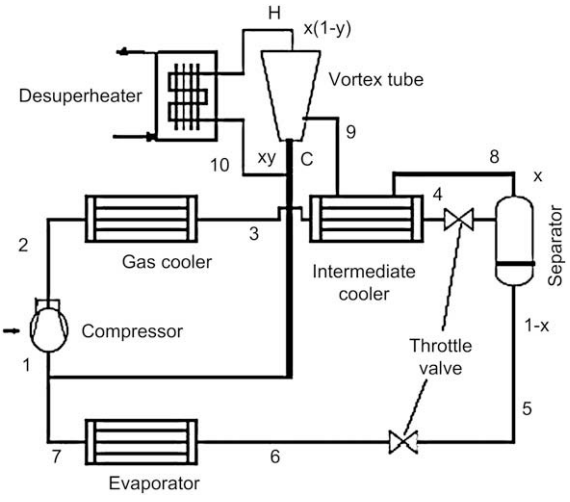


**Fig. 3.** Cycle layout of vortex tube expansion cycle for Keller model.

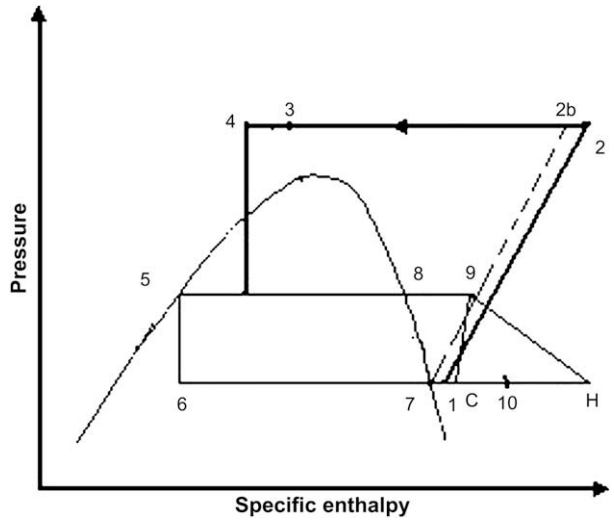


**Fig. 4.** p-h diagram of vortex tube expansion cycle for Keller model.

generation term [4], which may not practically feasible. Hence, due to individual difficulties of existing thermodynamic models for the vortex tube, a very simple model has been proposed and used in the present theoretical analysis of a vortex tube. The following assumptions have been made for the analysis:

(i) Negligible pressure drop in all heat exchangers and the connection tubes.
(ii) Both mixing and separation processes are isobaric.
(iii) No heat loss/gain with the environment, except with fluids for cooling purpose.
(iv) The refrigerant condition at the evaporator outlet is dry saturated.
(v) The compression process is adiabatic but non-isentropic.
(vi) All the kinetic energies at the nozzle exit in the vortex tube are absorbed by the warm fluid only.

Using these assumptions, the equations for the vortex tube expansion transcritical $CO_2$ cycle were setup. Based on the theoretical model, the simulation code was developed to investigate the effect of different operating parameters for both layouts, which was integrated with the thermodynamic property code CO2PROP [10], developed based on the Span and Wagner equations [11], to compute the relevant thermodynamic properties of carbon dioxide.

For given compressor discharge pressure, evaporator and gas cooler exit temperatures and component efficiencies, simulation procedures are described below:

For Maurer model, properties at 3, 4 and C are calculated from property code. The enthalpy at the vortex tube nozzle exit for given nozzle efficiency can be calculated by:

$$h_{3'} = h_3 - \eta_n[h_3 - h(p_{ev}, s_3)] \quad (1)$$

Then the vapor quality is found by $x = x(p_{ev}, h_{3'})$ using property code. Assuming that all the liquid $(1-x)$ is separated out and some fraction $(x^*y)$ of saturated vapor is separated as cold fluid, and rest $(x^*[1-y])$ absorbs all the kinetic energies and separated as hot fluid, properties at the hot end is given by,

$$h_H = (h_3 - (1-x)h_4 - xyh_C)/(x[1-y]) \quad (2)$$

$$t_H = t(p_{ev}, h_H) \quad (3)$$

Inlet enthalpy of evaporator can be found by,

$$h_6 = ([1-x]h_4 + xyh_C)/(1-x+xy) \quad (4)$$

State 5 can be found by using the effectiveness of desuperheater,

$$t_5 = t_H - \varepsilon(t_H - t_{wi}) \quad (5)$$

$$h_5 = h(p_{ev}, t_5) \quad (6)$$

The inlet of the compressor is found by,

$$h_1 = (1-x+xy)h_7 + x(1-y)h_5 \quad (7)$$

For the Keller model, properties at points 5 and 8 are evaluated using given intermediate pressure. Vapor quality and properties of points 4 and 9 are found by the iteration process using property code and following equations:

$$\varepsilon = (t_9 - t_8)/(t_3 - t_8) \quad (8)$$

$$h_3 - h_4 = x(h_9 - h_8) \quad (9)$$

$$x = (h_3 - h_5)/(h_8 - h_5) \quad (10)$$

For given nozzle efficiency, similar to Eq. (1), enthalpy at state C can be calculated by:

$$h_C = h_9 - \eta_n(h_9 - h(p_{ev}, s_9)) \quad (11)$$

Properties at the hot end are given by,

$$h_H = (h_9 - yh_C)/(1-y) \quad (12)$$

$$t_H = t(p_{ev}, h_H) \quad (13)$$

State 10 can be found by using the effectiveness of heat exchanger as similar to Eqs. (5 and 6). Then the inlet of the compressor is found by,

$$h_1 = (1-x)h_7 + xyh_C + x(1-y)h_{10} \quad (14)$$

The compressor outlet properties for both models are evaluated by using property code and given compressor isentropic efficiency.

The specific compressor work is given by,

$$w_c = h_2 - h_1 \quad (15)$$

The cooling output for the Maurer model and the Keller model, respectively, are given by,

$$q_{ev\_\mathrm{Maurer}} = (1-x+xy)(h_7 - h_6) \quad (16)$$

$$q_{ev\_\mathrm{Keller}} = (1-x)(h_7 - h_6) \quad (17)$$

The COPs of vortex tube expansion cycles and corresponding basic cycle have been evaluated by,

$$\mathrm{COP}_{\mathrm{Maurer}} = q_{ev\_\mathrm{Maurer}}/w_c \quad (18)$$

$$\mathrm{COP}_{\mathrm{Keller}} = q_{ev\_\mathrm{Keller}}/w_c \quad (19)$$

$$\mathrm{COP}_b = (h_7 - h_3)/(h_{2b} - h_7) \quad (20)$$

The COP improvements using vortex tube have been evaluated by,

$$\Delta\mathrm{COP}_{\mathrm{Maurer}} = (\mathrm{COP}_{\mathrm{Maurer}} - \mathrm{COP}_b)/\mathrm{COP}_b \quad (21)$$

$$\Delta\mathrm{COP}_{\mathrm{Keller}} = (\mathrm{COP}_{\mathrm{Keller}} - \mathrm{COP}_b)/\mathrm{COP}_b \quad (22)$$

## 4. Results and discussion

The performances of vortex tube expansion transcritical $CO_2$ cycle for both layouts have been evaluated at the optimum discharge pressure, corresponding to the maximum COP, for various evaporator temperature (−20 °C to 10 °C) and gas cooler exit temperature (30–60 °C). As discussed earlier, the optimum high-side pressure (or pressure drop) can be controlled by adjusting geometric parameters, which is generally done by cone valve [3] or by controlling needle valves [4] used at all vortex tube outlets. Cold mass fraction is also dependent on vortex tube design [3]. Hence, cold mass fraction and high-side pressure can be controlled simultaneously by adjusting geometric parameters and needle valves. The following input parameters have been taken for the study: heat exchanger effectiveness = 85%, expansion nozzle efficiency = 80%, compressor isentropic efficiency = 75% and the intermediate pressure = 5.7 MPa, which is the optimum value to get maximum COP improvement found by previous study [4]. Unless otherwise specified, the values of cold mass fraction of vortex tube and water inlet temperature are taken as 0.5 and 27 °C, respectively for the analysis. It may be noted that the cycle performances with high-side pressure optimizations have been presented in this study for given vortex tube efficiency, which may be defined as the multiplication of nozzle efficiency and cold mass fraction of vortex tube.

Results show that there is no effect of cold mass fraction and inlet water temperature of desuperheater on the optimum discharge pressure, although the minor effect of inlet water temperature have been observed for the Keller model (0.05 MPa per 10 °C). This is due to the fact that the optimum discharge pressure mainly depends on gas cooler exit temperature and evaporator temperature [10], which are invariant. The effect of cold mass fraction for water inlet temperature of 27 °C and inlet water temperature for cold mass fraction of 0.5 are shown in Fig. 5 at the optimum discharge pressure for the evaporator temperature of 5 °C and gas cooler outlet temperature of 40 °C. Results show that the effect of cold mass fraction is more significant for the Maurer model due to more pressure drop in the nozzle (higher pressure drop forms more amount of kinetic energy, which is absorbed by hot gas and rejected through the desuperheater) than the Keller model. With the increase in cold mass fraction, the COP improvement increases due to increase in heat rejection through the heat exchanger and for the same reason the COP improvement increases with the decrease in inlet water temperature. Maurer model can give more COP improvement than Keller model due to high heat rejection though heat exchanger or desuperheater for the given conditions.

The variations of optimum compressor discharge pressure and corresponding maximum cooling COP with refrigerant temperature at gas cooler exit are shown in Figs. 6 and 7 respectively, for the Maurer model at different evaporator temperatures for cold mass fraction of 0.5 and water inlet temperature of 27 °C. Results show that the optimum discharge pressure varies from 7.4 to 17.3 MPa, whereas the maximum cooling COP varies from 0.86 to 4.96 for the given ranges of evaporator and gas cooler outlet temperatures and the variations are very similar to the basic valve expansion cycle [10]. It may be noted that the optimum discharge pressure for gas cooler exit temperature of subcritical range (30–31 °C) is higher than corresponding saturation pressure [12]. Variation clearly shows that the effect of gas cooler exit temperature are much more significant compared to the evaporator temperature on the optimum discharge pressure where as equally significant on maximum cooling COP. Effect of evaporation temperature on optimum discharge pressure is more predominant at higher gas cooler outlet temperature, whereas reverse trend for maximum cooling COP. So the design of system for lowest possible gas cooler exit temperature and the highest possible evaporator temperature is more effective for not only maximum system COP also for lower optimum high-side pressure.

Fig. 8 shows the variation of cooling COP improvement over the basic cycle for the Maurer model at different evaporator temperatures. It may be noted that COP improvement varies from 0.3% to 18.7% for the given ranges. For the increase of gas cooler exit temperature or decrease of evaporation temperature, as the optimum discharge pressure increases, the vapor quality increases and hence for the constant cold mass fraction, mass flow rate through the desuperheater increases and the heat loss though desuperheater increases for given water inlet temperature, which lead to more COP improvement. However the effect of gas cooler

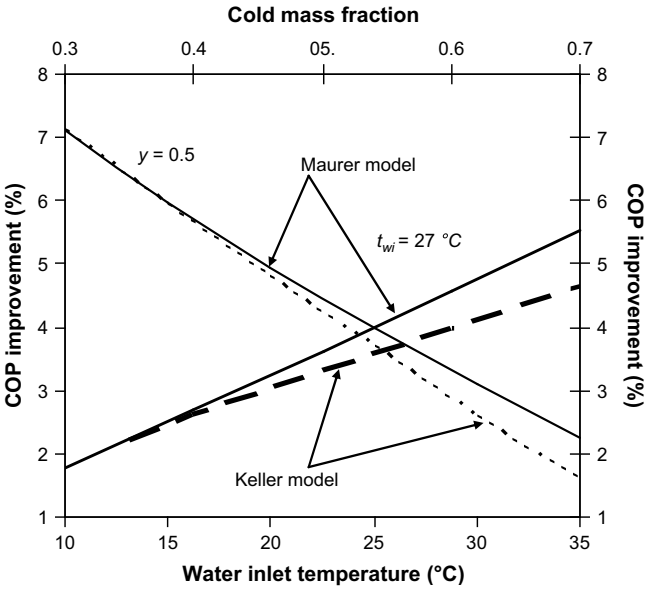


**Fig. 5.** Effect of $y$, $t_{wi}$ on the COP improvement.

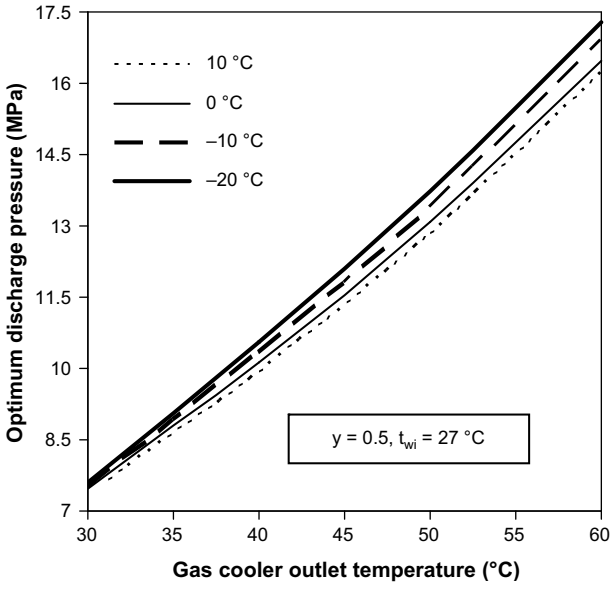


**Fig. 6.** Variation of optimum discharge pressure for Maurer model at different evaporation temperatures.

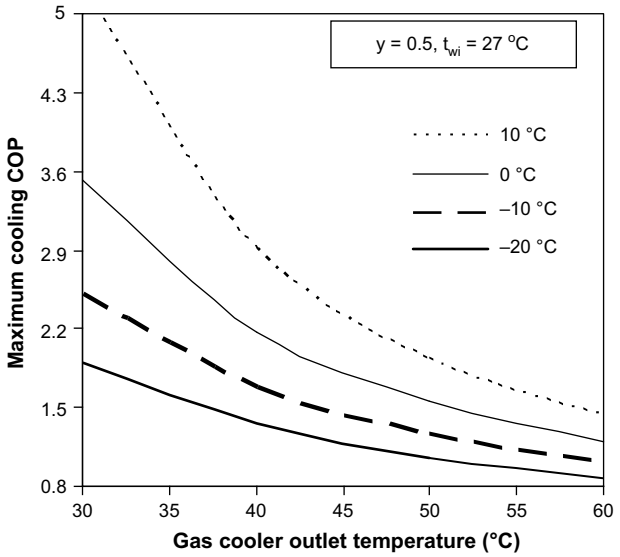


**Fig. 7.** Variation of maximum cooling COP for Maurer model at different evaporation temperatures.

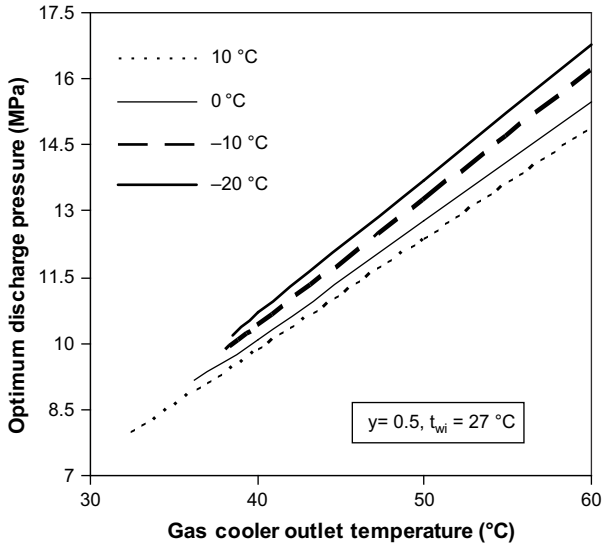


**Fig. 9.** Variation of optimum discharge pressure for Keller model at different evaporation temperatures.

exit temperature is more predominant than that of evaporation temperature due more effect on optimum discharge pressure as well as vapor quality. For the high temperature lift, the use of vortex tube is more effective in terms of higher COP improvement, lower expansion loss and higher reduction of optimum discharge pressure compared to basic cycle.

The variation of optimum compressor discharge pressure and corresponding maximum cooling COP with gas cooler exit temperature at different evaporator temperatures for cold mass fraction of 0.5 and water inlet temperature of 27 °C are shown in Figs. 9 and 10 respectively for the Keller model. It may be noted that the variation trends are similar as for the Maurer model, although both the optimum discharge pressure and maximum cooling COP give lower values (maximum of 2% and 6% respectively). Void portion in the both figures indicates that the vortex tube is not useful at that lower gas cooler exit temperature for given evaporator temperatures and it is possible to achieve higher COP with the baseline cycle. Similar to the Maurer model, the effect of gas cooler exit temperature are more significant compared to the evaporator temperature on the optimum discharge pressure whereas equally significant on maximum cooling COP. Results indicate that the design of system for lowest possible gas cooler exit temperature and the highest possible evaporator temperature is profitable in terms of system COP as well as lower optimum discharge pressure.

The variation of COP improvement over the basic cycle corresponding to optimum discharge pressure for Keller model is shown in Fig. 11 at different evaporator temperatures, where COP improvement varies from 0 to 17.8%. Variations show that the COP improvement increases as both the gas cooler exit and evaporator temperature increase. For the increase of gas cooler outlet temperature as the optimum discharge pressure increases, the vapor quality increases and hence the mass flow rate through the heat exchanger increases, which lead to more COP improvement, as similar to the Maurer model. However, the trend is opposite for the

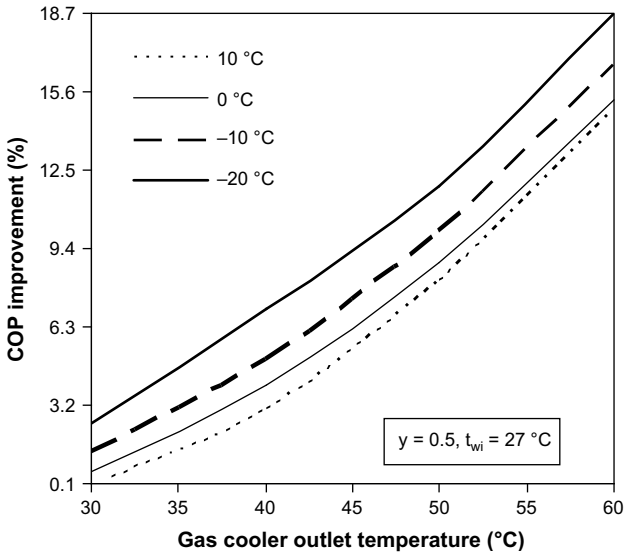


**Fig. 8.** COP improvement for Maurer model at different evaporation temperatures.

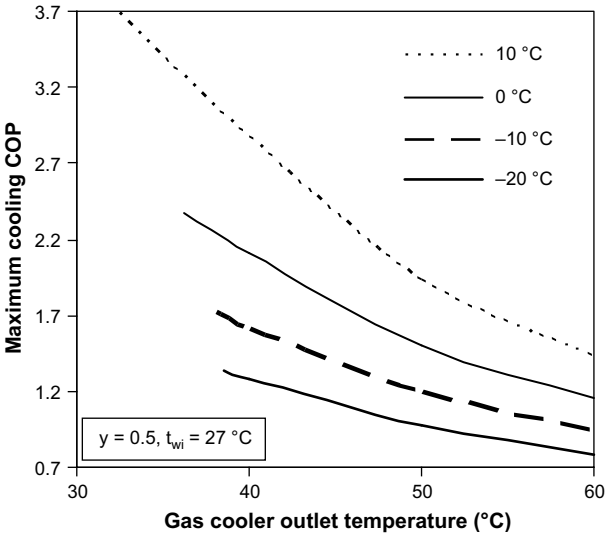


**Fig. 10.** Variation of maximum cooling COP for Keller model at different evaporation temperatures.

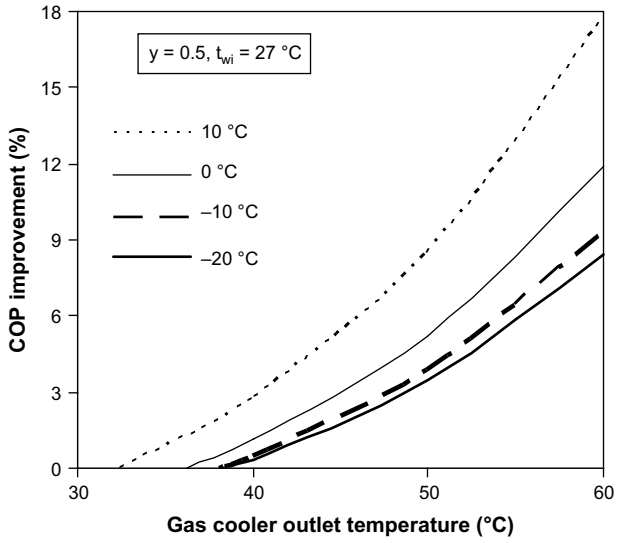


**Fig. 11.** COP improvement for Keller model at different evaporation temperatures.

evaporator temperature. This can be attributed that the vapor quality increases with the increase in evaporator temperature as the corresponding optimum discharge pressure decreases for the fixed intermediate pressure and certain gas cooler exit temperature. For the constant cold mass fraction, mass flow rate through the heat exchanger increases with increase in vapor quality and the heat loss though heat exchanger increases for given water inlet temperature and hence the COP improvement increases with increase in evaporation temperature. Deviation of optimum discharge pressure by use of vortex tube compared to that of basic cycle increases with increase in gas cooler exit temperature; however the effect of evaporation temperature is negligible. It may be noted that the modified Keller model, used in this study, gives more COP improvement (>2%) compared to original one.

Results show that the optimum discharge pressure is only dependent on evaporation and gas cooler exit temperatures, effect of other parameters (cold mass fraction, cold water inlet temperature, and isentropic efficiencies) are negligible. Performing a regression analysis on the data obtained from the cycle simulation, the following relations have been established to predict estimates the optimum discharge pressure (in MPa) for Maurer model ($R^2 = 99.6\%$) and Keller model ($R^2 = 99.5\%$), given in Eqs. (23 and 24), respectively,

$$p_{d,opt} = 1.077 - 0.0238 t_{ev} + 0.16 t_{co} + 0.00164 {t_{co}}^2 \quad (23)$$

$$p_{d,opt} = 1.605 - 0.0405 t_{ev} + 0.1653 t_{co} + 0.00115 {t_{co}}^2 \quad (24)$$

Where, $R^2$ signifies perfectness of data fitting and temperature in °C. These correlations are valid for the ranges of the evaporator temperature from −20 to 10 °C and the gas cooler exit temperature from 30 to 60 °C for the Maurer model however from $35.2 - 0.2\, t_{ev}$ to 60 °C (excluding the range, where vortex tube is useless) for the Keller model. It can be noted that the Maurer model gives moderately higher COP improvement than Keller model for given ranges. Study shows that the COP improvement increases with the decrease in evaporation temperature for the Maurer model, whereas the trend is reverse for the Keller model. Hence, the Maurer model can give higher COP improvement for lower cooling temperature applications.

## 5. Conclusions

Optimization of discharge pressure for vortex tube expansion transcritical $CO_2$ cycle based on the Maurer model as well as the Keller model, followed by COP improvement and effect on optimum discharge pressure using vortex tube are presented using a simple thermodynamic model. Negligible effect of cold mass fraction (or vortex tube efficiency) and inlet water temperature of heat exchanger on the optimum discharge pressure has been observed. Result shows that the effect of gas cooler exit temperature is more significant compared to the evaporator temperature on the optimum discharge pressure whereas equally significant on maximum cooling COP for both models. However the applicable range of vortex tube is less for the Keller model.

The use of vortex tube for Maurer model is more effective for higher temperature lift in terms of higher COP improvement and lower optimum discharge pressure over the basic cycle. For Keller model, effect of gas cooler exit temperature is similar to Maurer model, however, the improvement trend is opposite for the evaporator temperature. Maurer model can give moderately more COP improvement than Keller model and lower cost due less system components. The expansion loss also decreases significantly by use of vortex tube. Expressions for optimum discharge pressure for both cycle models have been developed and these correlations offer useful guidelines for optimum system design and selecting appropriate operating conditions.

## References

[1] E.A. Groll, Recent advances in the transcritical CO2 cycle technology, in: 8th National & 7th ISHMT-ASME Heat & Mass Transfer Conference, IIT Guwahati India, 2006.
[2] E.A. Groll, J.H. Kim, Review of recent advances toward transcritical $CO_2$ cycle technology, HVAC & R Research 13 (3) (2007) 499–520.
[3] S. Eiamsa-ard, P. Promvonge, Review of Ranque–Hilsch effects in vortex tubes, Renew. Sustain. Energ. Rev. 12 (7) (2008) 1822–1842.
[4] K.G. Christensen, M. Heiredal, M. Kauffeld, P. Schneider, Energy savings in refrigeration by means of a new expansion device, Report of Energy research programme, Journal no. 1223/99–0006 (2001).
[5] F.C. Hooper, C.W. Ambrose, Improved expansion process for the vapor refrigeration cycle, SAE preprints (1973) pp. 811–812.
[6] R.L. Collins, R.B. Lovelace, Experimental study of two-phase propane expanded through the Ranque–Hilsch tube, ASME J. Heat Transfer 101 (5) (1979) 300–305.
[7] D. Li, J.S. Baek, E.A. Groll, P.B. Lawless, Thermodynamic analysis of vortex tube and work output expansion devices for the transcritical carbon dioxide cycle, in: Fourth IIR-Gustav Lorentzen Conference on Natural Working Fluids at Purdue, Purdue University, USA, 2000, pp. 433–440.
[8] T. Maurer, Patent DE 197 48 083 A1, Entspannungseinrichtung, 1999.
[9] J. Keller, M. Göbel, Die thermodrossel: eine anlage zur entspannung komprimierter flüssigkeiten unter wärmeabgabe, Ki Luft-und Kältetechnik 2 (1997) 57–60.
[10] J. Sarkar, S. Bhattacharyya, M. Ramgopal, Optimization of a transcritical $CO_2$ heat pump cycle for simultaneous cooling and heating applications, Int. J. Refrigeration 27 (8) (2004) 830–838.
[11] R. Span, W. Wagner, A new equation of state for carbon dioxide covering the fluid region from triple point temperature to 1100 K at pressure up to 800 MPa, J. Phys. Chem. Ref. Data 25 (1996) 1509–1596.
[12] J. Sarkar, S. Bhattacharyya, M. Ramgopal, Natural refrigerant-based subcritical and transcritical cycles for high temperature heating, Int. J. Refrigeration 30 (1) (2007) 3–10.